Rotational cooling of molecular ions through laser-induced coupling to the collective modes of a two-ion Coulomb crystal

2006 J. Phys. B: At. Mol. Opt. Phys. 39 S1267

(http://iopscience.iop.org/0953-4075/39/19/S32)

INSTITUTE OF PHYSICS PUBLISHING JOURNAL OF PHYSICS B: ATOMIC, MOLECULAR AND OPTICAL PHYSICS

J. Phys. B: At. Mol. Opt. Phys. **39** (2006) S1267–S1280 doi:10.1088/0953-4075/39/19/S32

Rotational cooling of molecular ions through laser-induced coupling to the collective modes of a two-ion Coulomb crystal

I S Vogelius[1], **L B Madsen**[1] **and M Drewsen**[1,2]

[1] Department of Physics and Astronomy, University of Aarhus, 8000 Århus C, Denmark
[2] QUANTOP—Danish National Research Foundation Center for Quantum Optics, Department of Physics and Astronomy, University of Aarhus, 8000 Århus C, Denmark

Received 27 March 2006
Published 25 September 2006
Online at stacks.iop.org/JPhysB/39/S1267

Abstract

We show that the rotational degree of freedom of a polar heteronuclear molecular ion can be cooled through an optical coupling to the collective motional modes of the molecular ion and a simultaneously trapped and laser cooled atomic ion. Since the dissipative part of the rotational cooling is realized through laser cooling of the two-ion systems motional modes, the scheme should be applicable to a large range of molecules. As a test case for our cooling scheme we consider rotational cooling of a MgH^+ ion trapped with a laser cooled $^{40}Ca^+$ ion.

1. Introduction

Molecules are more difficult to cool than atoms because the multitude of ro-vibrational energy levels does not generally lead to a closed optical pumping cycle needed for conventional laser cooling. Having a translationally and internally cold molecular sample is, however, very attractive because the preparation of the system in a unique quantum state holds the promise for, for example, investigations of controlled chemical reactions and applications in quantum information science. For these reasons, a number of alternative cooling methods including Stark deceleration and buffer gas cooling have recently been developed (Bethlem and Meijer 2003, Doyle *et al* 2004, Egorov *et al* 2002). For molecular ions, the ability to cool the *translational degrees of freedom* has been thoroughly verified experimentally (Babab and Waki 1996, van Eijkelenborg *et al* 1999, Mølhave and Drewsen 2000, Blythe *et al* 2005, Drewsen *et al* 2004). For a trapped molecular ion, the large difference in energy scale between translational energy levels of the external motion in the trap (∼MHz) and internal molecular ro-vibrational energy levels ($\gtrsim 10^{11}$ Hz), led us in previous work (Vogelius *et al* 2002) to the assumption that the internal degrees of freedom would be unaffected by the translational cooling. A recent experiment by Bertelsen *et al* (2006), in which a lower bound on the rotational temperature of MgH^+ was found, supports this assumption. If, on the other hand,

a controllable explicit coupling mechanism is introduced, this situation can be changed, and in the case of trapped atomic ions, it has been proven both theoretically and experimentally that the coupling of internal and external degrees of freedom can successfully be exploited for cooling (Wineland and Itano 1979, Monroe *et al* 1995). Recently, this coupling has been applied in the construction of quantum gates as proposed by Cirac and Zoller (1995) and Sørensen and Mølmer (1999) and as implemented by Leibfried *et al* (2003) and Schmidt-Kaler *et al* (2003).

In the present paper, we show that similar mechanisms, that is controlled coupling between internal molecular and external motional states, can be exploited to cool internal and external degrees of freedom in molecular ions. The paper is organized as follows. In section 2, we present the basics of the scheme for cooling of the internal degree of freedom of the molecular ion. In section 3, we consider in detail the sympathetic translational cooling of a molecular ion by a laser cooled atomic ion. In section 4, we present the dynamics of the two-ion system during a laser-induced process where a Raman pulse connects electronic states of Σ symmetry. In section 5, we present the results of the cooling at longer times ($\sim$seconds) when the redistribution of population induced by black-body radiation becomes effective. In section 6, we discuss some of the complications of the proposed scheme, as well as prospects for improvement. Finally, in section 7, we conclude.

2. Scheme for rotational cooling

The cooling concept is illustrated in figure 1. In addition to the states of collective vibrations in the trap discussed above, the cooling scheme involves the molecular electronic ground state, $|g\rangle_{\rm el}$, an optically accessible excited electronic state of the molecule, $|e\rangle_{\rm el}$, and a number of rotational sub-states of the electronic molecular states, $|J\rangle_{\rm rot}$, with J being the rotational quantum number. We assume that the state $|\Psi\rangle$ of the system can be written as a product of these molecular states and the states of collective vibrations in the trap, i.e.,

$$|\Psi\rangle = |\psi\rangle_{\rm el}|J\rangle_{\rm rot}|\nu_{\rm CM}\rangle|\nu_{\rm BR}\rangle, \qquad |\psi\rangle_{\rm el} = (|e\rangle_{\rm el}, |g\rangle_{\rm el}), \tag{1}$$

where $|\nu_{\rm BR}\rangle$ and $|\nu_{\rm CM}\rangle$ denote the states of the breathing (BR) mode and centre of mass (CM) mode, respectively. The internal vibrational state is left out of the wavefunction $|\Psi\rangle$ since this degree of freedom is frozen out at room temperature for light molecules. Similarly in our specification of the state of the system, we ignore the atomic state which is not directly affected by the molecular cooling cycle.

Since the rotational energy $\frac{BJ(J+1)}{\hbar} \equiv \omega_{\rm rot}$ with B the rotation constant and J the rotational quantum number, is much larger than the typical energy in the external modes $\overline{\nu_p}\Omega_p$ ($p = $ BR, CM), the system can be considered a collection of rotational molecular states with sub-states of vibrational motion in the trap. These external vibrational states of one of the modes are shown in figure 1 as solid horizontal lines and the molecular part of the wavefunction is also indicated in the figure. The molecular rotational energy levels decouple from the external vibrational states in the trap without the application of an explicit coupling mechanism and the total population is therefore distributed over rotational levels as a Boltzmann distribution at room temperature (Bertelsen *et al* 2006). The equilibrium distribution of population for the lowest rotational states is schematically depicted as filled areas (blue online) superimposed on the states in figure 1 with the total area in each of the molecular rotational states proportional to the population in that state. The atomic Doppler cooling rates between external vibrational states in the trap, $\{\Gamma_{\rm atom}\}$ (see section 3), result in an equilibrium distribution over external vibrational levels in the trap potential with a temperature in the mK regime, in contrast to the room temperature distribution over rotational levels. The distribution of population over the

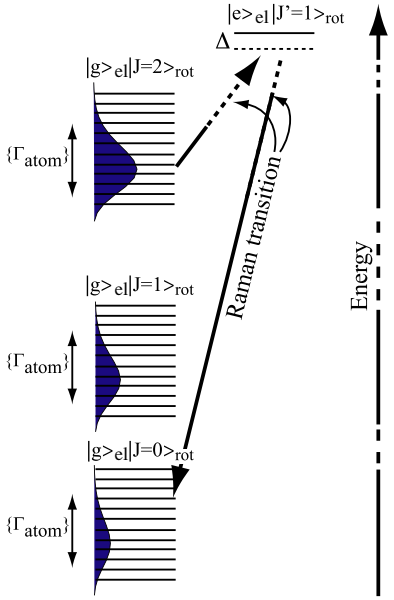

Figure 1. The proposed scheme is based on a Raman transition between two rotational states of the molecule, $|J=2\rangle_{\rm rot}$ and $|J=0\rangle_{\rm rot}$, both in the molecular electronic ground state, $|g\rangle_{\rm el}$. The sub-states of collective motion in the trap potential are depicted as solid horizontal lines. The equilibrium distribution without molecular cooling is a Boltzmann distribution over the sub-states of collective motion with mK temperature superimposed on a distribution over rotational levels at room temperature as explained in the text. The resulting distributions without molecular cooling are schematically shown as the filled areas with the population along the horizontal axis. Assuming that both the ground and excited electronic potentials have Σ symmetry, the Raman lasers are chosen to be resonant with states of collective motion in $|J=2\rangle_{\rm rot}$ and higher-lying motional states in $|J=0\rangle_{\rm rot}$ via an excited electronic state of the molecule $|e\rangle_{\rm el}$ with detuning Δ. The transitions between the rotational levels within the electronic ground state are mediated by spontaneous emission and black-body radiation (not shown in the figure). The continuous distributions depicted by the filled areas are schematic only; the physical distributions are discrete.

(This figure is in colour only in the electronic version)

external vibrational motional sub-states is thus peaked at a low vibrational quantum number, as shown in figure 1.

Assuming Σ symmetry of both involved electronic potentials, an effective coupling between the external vibrational modes and the internal rotations of the molecule is achieved by addressing the states, $|\Psi_i\rangle = |g\rangle_{\rm el}|J=2\rangle_{\rm rot}|\nu_{\rm CM}\rangle|\nu_{\rm BR}\rangle$, with a Raman transition which couples to $|\Psi_f\rangle = |g\rangle_{\rm el}|J=0\rangle_{\rm rot}|\nu'_{\rm CM}\rangle|\nu'_{\rm BR}\rangle$ with $\nu'_p > \nu_p (p = {\rm CM}, {\rm BR})$ via the excited electronic molecular state, $|\Xi_m\rangle = |e\rangle_{\rm el}|J=1\rangle_{\rm rot}|\nu''_{\rm CM}\rangle|\nu''_{\rm BR}\rangle$. The population in $|\Xi_m\rangle$ is maintained negligible through a large detuning. If we choose the Raman transition resonant with a state ν'_p with $\nu'_p - \nu_p \gg \bar{\nu}_p$, where $\bar{\nu}_p$ is the mean vibrational quantum number of the vibrational mode p, the population in $|J=2\rangle_{\rm rot}$ can be transferred to high-lying external vibrational states in $|J=0\rangle_{\rm rot}$. Population within the equilibrium distribution over vibrational levels with $|J=0\rangle_{\rm rot}$ can, however, not be transferred to $|J=2\rangle_{\rm rot}$ as the Raman transition will be detuned below the vibrational ground state $|g\rangle_{\rm el}|J=2\rangle_{\rm rot}|\nu_{\rm CM}=0\rangle|\nu_{\rm BR}=0\rangle$. We then conclude that population transferred from $|J=2\rangle_{\rm rot}$ to $|J=0\rangle_{\rm rot}$ will relax to the equilibrium distribution over vibrational levels in $|J=0\rangle_{\rm rot}$ from where it cannot be transferred back to $|J=2\rangle_{\rm rot}$. We have then established *unidirectional* pumping between the two molecular

states where the only dissipative term originates in the spontaneous decay of the atomic cooling cycle. We have previously shown that, with unidirectional pumping established, black-body radiation (BBR) can be used to cool the remaining rotational degrees of freedom in the molecule (Vogelius *et al* 2002, 2004a, 2004b). Unfortunately, the coupling matrix elements for $\nu'_p - \nu_p \gg \bar{\nu}_p$ are extremely small under realistic conditions. We will thus, through numerical simulations, show that effective unidirectional pumping is possible even when $\nu'_p - \nu_p < \bar{\nu}_p$. The coupling matrix elements are maximized if the lasers in the Raman process are chosen to be counter-propagating to ensure maximal momentum transfer.

In the next section we will derive the atomic cooling and heating rates, Γ_{atom}.

3. Sympathetic translational cooling of the molecular ion

3.1. Normal modes of the two-ion system

The derivation of the atomic cooling and heating rates is conveniently performed via the normal modes of the two-ion system. We consider the motion of a laser-cooled atomic ion and a sympathetically cooled heteronuclear diatomic molecular ion along one dimension of a harmonic trap. We assume the dynamics of the ions in the two other dimensions of the trap be decoupled from the motion considered here, thereby reducing the system to one dimension. The equation of motion can conveniently be written as a sum of two independent harmonic oscillator equations each representing a normal mode of collective vibration in the trap (Kielpinski *et al* 2000, James 1998). The modes in the trap are the centre of mass (CM) and the breathing (BR) mode, with vibrational states $|\nu_{\text{CM}}\rangle$ and $|\nu_{\text{BR}}\rangle$. To extract the cooling and heating rates due to the Doppler cooling of the atoms we need to keep track of the motion of the atoms only, and we therefore have to be able to extract the atomic degrees of freedom from the collective modes. The approach below is readily generalized to a string of N, but here we focus on one atomic and one molecular ion. The potential energy of the string of the atomic and the molecular ions both with nuclear charge q in the confining potential is given by (James 1998, Kielpinski *et al* 2000)

$$V = \frac{1}{2} q\phi_0 \left(x_{\text{at}}^2 + x_{\text{mol}}^2\right) + \frac{q^2}{4\pi\epsilon_0} \frac{1}{|x_{\text{at}} - x_{\text{mol}}|}. \tag{2}$$

Here x_m ($m = \text{at}, \text{mol}$) denotes the position of particle m and ϕ_0 is a constant describing the strength of the trap potential. The equilibrium positions of the ions in the confining potential can then be found by minimizing equation (2) with respect to x_m.

After Doppler cooling of the atomic ions, the displacement of the ions from the equilibrium positions is small, so we may write $x_m = x_m^0 + q_m(t)$, where x_m^0 is the equilibrium position of the mth ion and $\left|q_m(t)\right| \ll \left|x_{m+1}^0 - x_m^0\right|$. Following James (1998) and Kielpinski *et al* (2000), we now use the second-order expansion of the potential around the equilibrium positions to obtain an approximate expression for the Lagrangian,

$$L \approx \frac{1}{2} \sum_{m=1}^{2} M_m \dot{q}_m^2 - \frac{1}{2} \sum_{m,l=1}^{2} q_m q_l \left(\frac{\partial^2 V}{\partial x_m \partial x_l} \right) \tag{3}$$

$$= \frac{1}{2} \sum_{m=1}^{2} M_m \dot{q}_m^2 - \frac{1}{2} \phi_0 q \sum_{m,n=1}^{2} A_{n,m} q_n q_m \tag{4}$$

$$= \frac{1}{2} \sum_{m=1}^{2} \left(\frac{\mathrm{d}Q_m}{\mathrm{d}T} \right)^2 - \frac{1}{2} \sum_{m,n=1}^{2} A'_{n,m} Q_n Q_m, \tag{5}$$

where $Q_m = q_m\sqrt{\phi_0 q}$, $T = \sqrt{\phi_0 q/M_{\text{at}}}t$,

$$A_{n,m} = \begin{cases} 1 + 2\sum_{p\neq m}^{2} \dfrac{1}{|u_m - u_p|^3} & \text{if} \quad n = m \\ \dfrac{-2}{|u_m - u_n|^3} & \text{if} \quad n \neq m, \end{cases}$$

with $u_m = x_m^0 \big/ \sqrt[3]{q/4\pi\epsilon_0\phi_0}$, and

$$A'_{n,m} = \begin{cases} A_{n,m} & \text{if} \quad n = \text{at}, \quad m = \text{at} \\ \dfrac{A_{n,m}}{\sqrt{\mu}} & \text{if} \quad n = \text{mol}, \ m = \text{at} \vee m = \text{mol}, \ n = \text{at} \\ \dfrac{A_{n,m}}{\mu} & \text{if} \quad n = \text{mol}, \ m = \text{mol}, \end{cases}$$

with $\mu = \frac{M_{\text{mol}}}{M_{\text{at}}}$. In the derivation we used the fact that the equilibrium positions minimize the potential, resulting in a vanishing linear term in the Taylor expansion, and then neglected the constant term.

We find the eigenmodes of collective vibrations expressed in terms of Q_m by diagonalizing A', i.e., as the normalized eigenvectors $\mathbf{v}_k$ and eigenvalues ξ_k corresponding to the equation $A'\mathbf{v}_k = \xi_k^2\mathbf{v}_k$. Now, by expanding Q_m on the eigenvectors $\mathbf{v}_k$ we may write the Lagrangian of equation (3) in the basis of the eigenmodes, in which case it takes the form

$$L = \frac{1}{2}\sum_{p=1}^{2}\left(\frac{\mathrm{d}Q'_p}{\mathrm{d}T}\right)^2 - \frac{1}{2}\sum_{p=1}^{2}\xi_p^2 Q'^2_p, \tag{6}$$

where $Q'_p = \mathbf{v}_p \cdot \mathbf{Q}$. Equation (6) is immediately recognized as the Lagrangian of a superposition of 2 harmonic oscillators with frequencies ξ_p and unit mass (for the MgH^+, $^{40}Ca^+$ system studied below we have $\xi^2_{\text{CM}} = 1.0954$ and $\xi^2_{\text{BR}} = 2$).

We may now proceed to the quantization of the vibrational motion. From equation (6), the Hamiltonian of the system is found to be

$$H = \frac{1}{2}\sum_{p=1}^{2}P_p^2 + \frac{1}{2}\sum_{p=1}^{2}\xi_p^2 Q'^2_p, \tag{7}$$

with the P_p being the canonical momentum conjugate to Q'_p, i.e. $P_p = \dot{Q}'_p$. We make the operator substitution $P_p \to -\mathrm{i}\frac{\mathrm{d}}{\mathrm{d}Q'_p}$ and find $[Q'_p, P_q] = \mathrm{i}\delta_{pq}$. Defining ladder operators

$$a_p^{\pm} = \frac{1}{\sqrt{2}}\left(\sqrt{\xi_p}Q'_p \mp \frac{\mathrm{i}P_p}{\sqrt{\xi_p}}\right), \tag{8}$$

we find

$$H = \sum_p \xi_p\left(a_+^p a_-^p + \frac{1}{2}\right), \qquad \left[a_-^p, a_+^q\right] = \delta_{pq}. \tag{9}$$

As expected, the quantized Hamiltonian is a superposition of independent harmonic oscillator Hamiltonians. The physical eigenfrequencies of the vibrational modes are found by transforming $T \to t$ giving $\Omega_p = \xi_p\Omega_{\text{trap}}$. Similarly, the physical position coordinates of the ions can be found by transforming $Q'_p \to q_m$.

3.2. Atomic Doppler cooling rates, Γ_{atom}

Let us now simply assume that the atomic ion can be treated as a two-level system with a transition frequency ω_0 and a natural excited state lifetime of γ_{natural}, then if $\gamma_{\text{natural}} \gg \Gamma_{\text{CM,BR}}$ and $\hbar k^2/(2m) < \gamma_{\text{natural}}$, where k is the wave-number of the laser light, a semiclassical approach can be applied in calculating the cooling process (Metcalf and van der Straten 1999).

The cooling force on the atomic ion can in this approximation be written as

$$F = -2\alpha v_x^{\text{at}}, \tag{10}$$

where v_x^{at} is restricted to the single dimension under concern and where

$$\alpha = -\hbar k^2 \frac{s}{(s+1)^2} \frac{\Delta \gamma_{\text{natural}}}{\Delta^2 + \gamma_{\text{natural}}^2/4}, \tag{11}$$

with $\Delta = \omega_{\text{Laser}} - \omega_0$ being the detuning of the atomic ion cooling transition and s the saturation parameter

$$s = \frac{\Omega_{\text{Rabi}}^2/2}{\Delta^2 + \gamma_{\text{natural}}^2/4}, \tag{12}$$

with Rabi frequency Ω_{Rabi}. It follows from equation (10) that the change in the kinetic energy per unit time satisfies

$$\frac{\mathrm{d}E_{\text{kin}}^{\text{at}}}{\mathrm{d}t} = -\frac{4\alpha}{m_{\text{at}}} E_{\text{kin}}^{\text{at}}, \tag{13}$$

with $E_{\text{kin}}^{\text{at}} = p_{\text{at}}^2/2m_{\text{at}}$. We may express p_{at} in terms of normal modes. We have the following relation between physical q_{at} and the scaled coordinates $Q_{\text{at}} = q_{\text{at}}\sqrt{\phi}_0 q$, so $\mathrm{d}Q_{\text{at}}/\mathrm{d}q_{\text{at}} = \sqrt{\phi}_0 q$ and

$$p_{\text{at}} = \sqrt{\phi}_0 q \left(-\mathrm{i}\hbar \frac{\mathrm{d}}{\mathrm{d}Q_{\text{at}}}\right). \tag{14}$$

The scaled particle position Q_{at} is related to the eigenmodes via $Q'_p = \boldsymbol{v}_{p,\text{at}} \cdot Q$, i.e.,

$$Q_p = \sum_{m=\text{at,mol}} v_{p,m} Q_m, \tag{15}$$

where $p = \text{CM, BR}$. Since, now, $\mathrm{d}/\mathrm{d}Q_{\text{at}} = \sum_p (\mathrm{d}/\mathrm{d}Q'_p)(\mathrm{d}Q'_p/\mathrm{d}Q_{\text{at}}) = \sum_p v_{p,\text{at}}(\mathrm{d}/\mathrm{d}Q'_p)$ it follows from equation (14) that p_{at} is given in terms of normal mode $P'_p = -\mathrm{i}\hbar\sqrt{\phi q/m_{\text{at}}}\mathrm{d}/(\mathrm{d}Q'_p)$ operators as

$$p_{\text{at}} = \sqrt{m}_{\text{at}} \sum_p v_{p,\text{at}} P'_p. \tag{16}$$

By equation (8), the normal mode momentum operators are given by

$$P_p = \mathrm{i}\sqrt{\frac{\xi_p}{2}}\left(a_p^+ - a_p^-\right). \tag{17}$$

Using equations (16) and (17) we may now finally evaluate the right-hand side of equation (13) as the expectation value of the kinetic energy operator in the motional vibrational state $|\psi_{\text{vib}}\rangle = \prod_p |v_p\rangle$,

$$\langle E_{\text{kin,at}} \rangle = \frac{\hbar}{2} \sum_p v_{p,\text{at}}^2 \xi_p (v_p + 1/2) \tag{18}$$

Table 1. Typical absolute values of the atomic cooling and heating rates in Hz for the centre of mass (CM) and the breathing (BR) mode of the MgH^+–$^{40}Ca^+$ two-ion system.

Initial v_{CM}	$\Gamma^{cool}_{v_{CM}}$	$\Gamma^{heat}_{v_{CM}}$
0		2.5×10^4
1	4.1×10^4	2.5×10^4
2	6.8×10^4	2.5×10^4
3	9.5×10^4	2.5×10^4
Initial v_{BR}	$\Gamma^{cool}_{v_{BR}}$	$\Gamma^{heat}_{v_{BR}}$
0		1.4×10^4
1	1.6×10^4	1.4×10^4
2	2.7×10^4	1.4×10^4
3	3.8×10^4	1.4×10^4

and from equation (13) we obtain

$$\frac{dE^{at}_{kin}}{dt} = -\frac{2\alpha}{m_{at}}\Omega_{trap}\sum_p v^2_{p,at}\xi_p(v_p + 1/2), \tag{19}$$

or by the energy $E^{at}_{kin} = \hbar\Omega_{trap}\xi_p(v_p + 1/2)$,

$$\frac{dv_p}{dt} = -\frac{2\alpha}{m_{at}}v^2_{p,at}(v_p + 1/2), \tag{20}$$

Hence, the atomic cooling rate reads

$$\Gamma^{cool}_{v_p} = -\frac{2\alpha}{m_{at}}v^2_{p,at}(v_p + 1/2). \tag{21}$$

We now turn to a discussion of the heating rate. Fluctuations in the number of absorbed photons and recoil effects lead to a heating rate (Metcalf and van der Straten 1999)

$$\frac{dE_{heat}}{dt} = \frac{1 + 2/5}{4m}\hbar^2k^2\gamma_{natural}2s. \tag{22}$$

However, in terms of normal modes, $\frac{dE_{heat,p}}{dt} = d/(dt)\sum_p \hbar\Omega_p(v_p + 1/2)$. The atomic absorption rate is largely independent of the vibrational state of the atom, so we assume that $d/(dt)E^p_{heat}$ is independent of p, so (22) is equal to twice the mode-specific heating rate. We now translate into frequency and proceed with the quantization as above and find

$$\Gamma^{heat}_{v_p} = \frac{1 + 2/5}{4m_{at}\Omega_p}\hbar k^2\gamma_{natural}s. \tag{23}$$

The resulting temperature of the external vibrations in the trap is in the mK regime, and the corresponding distribution is, accordingly, peaked at low vibrational quantum number (see figure 1). Table 1 summarizes some typical cooling and heating rates for the MgH^+–$^{40}Ca^+$ two-ion system.

Even for $\gamma_{natural} \sim \Gamma_{CM,BR}$ the above approximation gives reasonable results, but when $\gamma_{natural} \ll \Gamma_{CM,BR}$, in the so-called re-solved sideband cooling regime, a full quantum mechanical treatment is needed.

4. Dynamics during Raman pulses: translational cooling and extraction of effective pumping rates

With the atomic cooling and heating rates at hand we now consider the dynamics under the Raman pulses. At the short (ms) time scale of the Raman pulse the evolution of the system due to the BBR can be safely neglected and the evolution is described by the rate equation

$$\frac{\mathrm{d}\mathbf{P}}{\mathrm{d}t} = K\mathbf{P}, \tag{24}$$

where $\mathbf{P}$ is a vector with population in the states $|g\rangle_{\mathrm{el}}|J\rangle_{\mathrm{rot}}|\nu_{\mathrm{CM}}\rangle|\nu_{\mathrm{BR}}\rangle$ and K is a coupling matrix determined by $\{\Gamma_{\mathrm{atom}}\}$ and the set of coupling rates between internal molecular states and external motion in the trap, $\{\Gamma_{\mathrm{mol}}\}$. The matrix K is partitioned into different J blocks corresponding to rotational quantum number $J = 0, 1$ and 2. Within each J block the atomic rates discussed in section 3 couple nearest neighbour states for both the CM and the BR modes. For the Σ states considered here, the Raman transition only couples the $J = 0$ and $J = 2$ levels. The evaluation of the accompanying rates $\{\Gamma_{\mathrm{mol}}\}$ proceeds as follows. The interaction operator describing the interaction of the molecule with the Raman pulse is $V_I = \mathbf{d}\cdot\mathbf{E}_1(x,t) + \mathbf{d}\cdot\mathbf{E}_2(x,t) = \frac{1}{2}V_I^{(1)}(\mathrm{e}^{\mathrm{i}k_1\hat{x}} + \mathrm{e}^{-\mathrm{i}k_1\hat{x}}) + \frac{1}{2}V_I^{(2)}(\mathrm{e}^{\mathrm{i}k_2\hat{x}} + \mathrm{e}^{-\mathrm{i}k_2\hat{x}})$ with $\mathbf{d}$ the dipole operator and $\mathbf{E}_l(x,t)$ the electric field from laser $l = (1,2)$ with frequency ω_l and wave number k_l. Assume that the frequency $\omega_1 + \Delta$ is resonant with the molecular transition $|g\rangle_{\mathrm{el}}|J=2\rangle_{\mathrm{rot}} \rightarrow |e\rangle_{\mathrm{el}}|J=1\rangle_{\mathrm{rot}}$ and that the frequency $\omega_2 + \Delta$ is resonant with the molecular transition $|e\rangle_{\mathrm{el}}|J=1\rangle_{\mathrm{rot}} \rightarrow |g\rangle_{\mathrm{el}}|J=0\rangle_{\mathrm{rot}}$. The transition rate induced by the interaction V_I from an initial state, $|\Psi_i\rangle = |g\rangle_{\mathrm{el}}|J=2\rangle_{\mathrm{rot}}\nu_{\mathrm{CM}}|\nu_{\mathrm{BR}}\rangle$, to a final state, $|\Psi_f\rangle = |g\rangle_{\mathrm{el}}|J=0\rangle_{\mathrm{rot}}|\nu'_{\mathrm{CM}}\rangle|\nu'_{\mathrm{BR}}\rangle$, via a collection of intermediate states, $|\Xi_m\rangle = |e\rangle_{\mathrm{el}}|J=1\rangle_{\mathrm{rot}}|\nu''_{\mathrm{CM}}\rangle|\nu''_{\mathrm{BR}}\rangle$, is then given by

$$\Gamma_{i\to f} = \frac{1}{4\hbar^4}\left|\sum_m \frac{\langle\Psi_f|V_I^{(2)}\,\mathrm{e}^{-\mathrm{i}k_2\hat{x}}|\Xi_m\rangle\langle\Xi_m|V_I^{(1)}\,\mathrm{e}^{\mathrm{i}k_1\hat{x}}|\Psi_i\rangle}{\frac{E_m-E_i}{\hbar} - \omega_1 - \frac{1}{2}\mathrm{i}\gamma_m}\right|^2 \mathcal{L}(\Gamma,\delta), \tag{25}$$

where E_i, E_m and E_f denote the energies of $|\Psi_i\rangle, |\Xi_m\rangle$ and $|\Psi_f\rangle$, respectively, γ_m is the line width of the intermediate state and we apply the rotating wave approximation and ignore far off-resonant terms. Furthermore, we have introduced a Lorentzian line-width function, $\mathcal{L}(\Gamma,\delta) = \frac{1}{\pi}\frac{\Gamma}{\delta^2+\Gamma^2}$ with $\delta = \omega_1 - \omega_2 - \frac{E_f-E_i}{\hbar}$ to describe the effect of a laser bandwidth Γ. The expression is simplified by denoting the molecular matrix element by $\Omega^{\pm}_{\mathrm{mol}_l} = \frac{1}{\hbar}\langle e|_{\mathrm{el}}\langle J=1|_{\mathrm{rot}}, V_I^{(l)}|J = J = 1\pm 1\rangle_{\mathrm{rot}}|g\rangle_{\mathrm{mol}}$

$$\Gamma_{i\to f} = \frac{1}{4}\left|\Omega^{+}_{\mathrm{mol}_2}\right|^2|\Omega^{-}_{\mathrm{mol}_1}|^2 \times \left|\sum_{\nu''_{\mathrm{CM}},\nu''_{\mathrm{BR}}} \frac{\langle\nu'_{\mathrm{CM}},\nu'_{\mathrm{BR}}|\,\mathrm{e}^{-\mathrm{i}k_2\hat{x}}|\nu''_{\mathrm{CM}},\nu''_{\mathrm{BR}}\rangle\langle\nu''_{\mathrm{CM}},\nu''_{\mathrm{BR}}|\,\mathrm{e}^{\mathrm{i}k_1\hat{x}}|\nu_{\mathrm{CM}},\nu_{\mathrm{BR}}\rangle}{\frac{E_m-E_i}{\hbar} - \omega_1 - \frac{1}{2}\mathrm{i}\gamma_m}\right|^2 \mathcal{L}(\Gamma,\delta), \tag{26}$$

where $\left|\Omega^{\pm}_{\mathrm{mol}_l}\right|^2$ can be expressed in terms of the Einstein A coefficient between the molecular states (Vogelius *et al* 2004a). All other molecular coupling matrix elements are negligible due to selection rules.

It remains to calculate the transition matrix elements between collective motional states in the trap. To this end, we recall the discussion of section 3 and use that $\hat{x} = x_0 + q_{\mathrm{CM}} + q_{\mathrm{BR}} = x_0 + \sum_p q_p$ to obtain

$$\langle\nu'_{\mathrm{CM}}\nu'_{\mathrm{BR}}|\,\mathrm{e}^{\mathrm{i}k\hat{x}}|\nu_{\mathrm{CM}}\nu_{\mathrm{BR}}\rangle = \mathrm{e}^{\mathrm{i}kx_0}\prod_p\langle\nu'_p|\,\mathrm{e}^{\mathrm{i}kq_p}|\nu_p\rangle. \tag{27}$$

The first factor is just an overall phase factor that cancels out. The two factors in the product over normal modes p are by now standard matrix elements in quantum optics text books and in the context of laser cooling they were calculated by Wineland and Itano (1979).

The computational task is made considerably less demanding by making approximations as follows. The eigenenergies of the excited states $|\Xi_m\rangle$ are given by $E_m = \hbar\omega_{ge} + \hbar\Omega_{\mathrm{CM}}\left(\nu''_{\mathrm{CM}} + \frac{1}{2}\right) + \hbar\Omega_{\mathrm{BR}}\left(\nu''_{\mathrm{BR}} + \frac{1}{2}\right)$, where ω_{ge} denotes the free molecule transition frequency. For reasonable detuning from the excited electronic molecular state, $\Omega_{\mathrm{CM}}\left(\nu''_{\mathrm{CM}} + \frac{1}{2}\right) + \Omega_{\mathrm{BR}}\left(\nu''_{\mathrm{BR}} + \frac{1}{2}\right) \ll \omega_{ge} - \omega_1$. Furthermore, we assume that the linewidth of $|\Xi_m\rangle$ is independent of the motional excitations, i.e., $\gamma_m \simeq \gamma_{\mathrm{natural}}$. Under these assumptions, the denominator in equation (26) is independent of m. We may then use completeness of the collective motional states, $\sum_{\nu_p} |\nu_p\rangle\langle\nu_p| = 1$, to completely eliminate the sum over intermediate states, thus reducing equation (26) to

$$\Gamma_{i\to f} = \frac{1}{4}|\Omega^{+}_{\mathrm{mol}_2}|^2|\Omega^{-}_{\mathrm{mol}_1}|^2\left|\frac{\langle\nu'_{\mathrm{CM}}\nu'_{\mathrm{BR}}|\,\mathrm{e}^{\mathrm{i}k_1\hat{x}-\mathrm{i}k_2\hat{x}}|\nu_{\mathrm{CM}}\nu_{\mathrm{BR}}\rangle}{\Delta - \frac{1}{2}\mathrm{i}\gamma_{\mathrm{natural}}}\right|^2\mathcal{L}(\Gamma,\delta). \tag{28}$$

Here, $\Delta = \omega_{ge} - \omega_1$ denotes the single photon detuning from the intermediate state. Note that equations (26) and (28) give results for the populations which cannot be distinguished on the scale of the figures below. It takes approximately 10 h on a standard PC to obtain the rates from equation (26) while equation (28) allows us to obtain the results in less than 3 min.

Our next task is to extract the effective rates for the $J = 0$ to the $J = 2$ transition and vice versa corresponding to the process shown in figure 1. The effective rates make no reference to all the external motional states, and hence a propagation of the dynamics over the timescale of seconds, necessary for the black-body radiation to become effective, becomes possible. We illustrate the effective-rate-extraction procedure with a calculation on the rotational cooling of MgH^+ though sympathetic Doppler laser cooling of a $^{40}Ca^+$ ion and by coupling the internal and external motions as described above. In our simulation of the Raman process, we neglect spontaneous decay processes and use an oscillation trap frequency of $\Omega_{\mathrm{Ca}} = 50$ MHz for the calcium ion. The transition rates in equations (26)–(28) are evaluated with $\nu_p, \nu'_p, \nu''_p = 0\cdots 40$, $p = (\mathrm{CM}, \mathrm{BR})$. The oscillation frequencies of the two external modes are $\Omega_{\mathrm{CM}} \simeq 50$ MHz and $\Omega_{\mathrm{BR}} \simeq 100$ MHz. We use the linewidth ($\gamma_{\mathrm{natural}} = 2\pi \times 22$ MHz) and transition wavelength ($\lambda = 397$ nm) of the $4s^2S_{1/2} - 4p^2P_{1/2}$ Doppler cooling transition in $^{40}Ca^+$. The Rabi frequency of the atomic cooling transition is chosen to be 50 MHz. The lasers in the Raman process were tuned to resonance when $\nu'_p - \nu_p = 2$. The coupling rate $\Omega^{\pm}_{\mathrm{mol}_i}$ was chosen to be 3 GHz for both transitions and the detuning from the excited state was 750 GHz. The width of the Lorentz function was chosen to $\Gamma = 1$ kHz, and the Raman coupling lasers were assumed to be pulsed with a pulse length of 1 ms. In our simulations we have included rates under the Lorentzian profile until convergence.

The initial distribution over collective motional states was the equilibrium distribution resulting from $\{\Gamma_{\mathrm{atom}}\}$ alone, while the molecule was assumed to be in $|J = 2\rangle_{\mathrm{rot}}$. We propagated the rate equations with this initial distribution of population for 1 ms. This is a short time scale for the rotational transitions within the molecular ground state potential.

The full curves in figure 2 show the population distribution at representative times during pumping. The dashed curves show the corresponding distribution without the Raman transition. We see as expected from the discussion in section 2 that the Raman transition results in an effective transfer of population from the initial $|J = 2\rangle_{\mathrm{rot}}$ molecular state to $|J = 0\rangle_{\mathrm{rot}}$ (see figure 1).

To exploit this population transfer for cooling, the state $J = 2$ has to be re-populated. This is where the black-body radiation comes in. The effect of the latter, however, sets in on much longer time scale (∼seconds). It is unwieldy to propagate the system of equations with

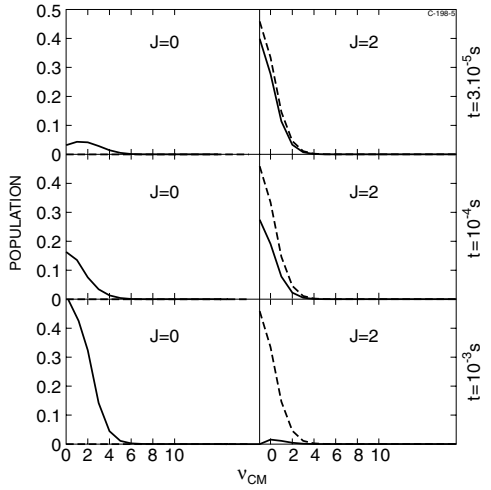

Figure 2. The distribution of the population in the CM mode of the collective motion in the trap potential at representative times during a Raman pulse. Population in $|J = 0\rangle_{\rm rot}$ is shown in the left half, while population in $|J = 2\rangle_{\rm rot}$ is depicted in the right. The simulation was started from $J = 2$ and with an equilibrium distribution over the external motional states resulting from atomic cooling. Full curves depict distributions with the Raman transition shown in figure 1, while dashed curves represent population distributions without the Raman transition. Results for the BR mode are very similar, except that the equilibrium distribution is shifted to the left due to the higher eigenfrequency of this mode.

all motional states included on such a time scale. We therefore fit the evolution of population to the solution of a system of two coupled differential equations corresponding to an effective pumping rate, $\gamma_{2\to0}$, pumping from $|J = 2\rangle_{\rm rot}$ to $|J = 0\rangle_{\rm rot}$ and another effective rate, $\gamma_{0\to2}$, pumping from $|J = 0\rangle_{\rm rot}$ to $|J = 2\rangle_{\rm rot}$. This gives a near-perfect fit with $\gamma_{2\to0} = 5.3 \times 10^3\ {\rm s}^{-1}$ and $\gamma_{0\to2} = 0.18 \times 10^3\ {\rm s}^{-1}$. Since the effective rate model accurately describes the effect of the Raman pulses we may exclude the external motional states from our basis of states and consider the long time dynamics with the effective rates above and the BBR induced transitions between the rotational states of relevance.

5. Long-time dynamics: black-body-induced rotational cooling

The rates $\gamma_{2\to0}$ and $\gamma_{0\to2}$ are now used to propagate rate equations representing a system of the lowest 12 rotational states labelled by $i = 0, 1, 2, \ldots, 11$ of MgH^+ when interacting with the 300 K black-body radiation (BBR) field present in the trap and subject to the presented cooling mechanism. In short the equation of motion of the molecular population P_i in state i reads

$$\begin{aligned}\frac{{\rm d}P_i}{{\rm d}t} = &-\sum_{j=0}^{i-1} A_{ij}P_i + \sum_{j=i+1}^{M} A_{ji}P_j - \sum_{j=0}^{i-1} P_i B_{ij} W(\omega_{ij}) + \sum_{j=0}^{i-1} P_j B_{ji} W(\omega_{ij}) \\ &- \sum_{j=i+1}^{M} P_i B_{ij} W(\omega_{ij}) + \sum_{j=i+1}^{M} P_j B_{ji} W(\omega_{ij}) \\ &+ \delta_{i,0}(\gamma_{2\to0}P_2 - \gamma_{0\to2}P_0) + \delta_{i,2}(\gamma_{0\to2}P_0 - \gamma_{2\to0}P_2). \end{aligned} \tag{29}$$

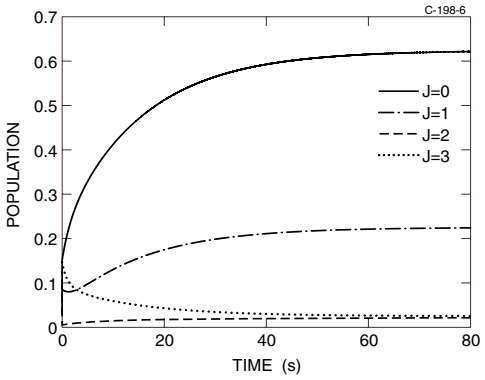

Figure 3. Population in the four lowest rotational states of MgH^+ as a function of time, when subject to the 300 K BBR field present in the trap and the cooling scheme shown in figure 1. The simulation was performed using effective rates for the pumping of population between $|J = 0\rangle_{\rm rot}$ (full curve) and $|J = 2\rangle_{\rm rot}$ (dashed curve) as explained in the text. The population in $|J = 2\rangle_{\rm rot}$ is rapidly emptied as a result of the large effective pumping rate $\gamma_{\rm cool}$, while the population in $|J = 3\rangle_{\rm rot}$ (dotted curve) is removed somewhat more slowly as the result of BBR redistributions. Finally, the population in $|J = 1\rangle_{\rm rot}$ (chained curve) increases as a result of rotational heating from the ground state. The population in the rotational ground state after 60 s is ∼60%, while the population in $|J = 0\rangle_{\rm rot}$ and $|J = 1\rangle_{\rm rot}$ combined is larger than 80%.

Here $M = 11$ is chosen such that the population in higher-lying rotational states is negligible during the cooling process. A_{ij} and B_{ij} are the Einstein coefficients describing spontaneous and stimulated transitions from energy level i to j. $W(\omega_{ij})$ is the BBR radiative energy density present in the trap at the resonant transition frequency $\omega = \omega_{ij}$, between levels i and j. The last terms describe the coupling due to the effective pumping rates $\gamma_{2\to0}$ and $\gamma_{0\to2}$ and $\delta_{i,0}$ and $\delta_{i,2}$ denote the Kronecker delta functions. The first term in equation (29) describes spontaneous decay from state i to states with lower energy, while the second term describes spontaneous decay from levels with higher energy into state i. Black-body-radiation stimulated emission from the ith state and BBR stimulated absorption from lower-lying states is then described by the third and fourth terms, and finally, the fifth and sixth terms represent transitions due to absorption of radiation from the ith state and stimulated emission from higher-lying states into the ith state. The Einstein coefficients of relevance for MgH^+ were given by Vogelius *et al* (2004a) and the numerical values for the pumping rates were given in the preceding section.

The result of an integration of the set of equations (29) is shown in figure 3. The simulation is performed with continuous pumping, which is a good approximation provided the repetition frequency of the Raman lasers is much faster than the BBR rotational redistribution rate.

The $J = 2$ level is emptied immediately due to the comparatively large $\gamma_{2\to0}$. The remaining rotational levels of the molecule are redistributed due to transitions mediated by BBR and spontaneous decays. After 60 s more than 60% of the distribution is found in the ground state. The only excited rotational state which is not emptied by $\gamma_{2\to0}$ and BBR induced rotational redistribution is $|J = 1\rangle_{\rm rot}$. This is explained as rotational heating from the highly populated $|J = 0\rangle_{\rm rot}$ in the presence of BBR at a timescale so fast that rotational heating from $|J = 1\rangle_{\rm rot}$ to $|J = 2\rangle_{\rm rot}$ cannot compensate. This effect can be somewhat reduced by the introduction of tailored incoherent fields as discussed by Vogelius *et al* (2004b). Even without the use of such fields we note that more than 80% of the total population is in the two lowest rotational states, roughly corresponding to a rotational temperature of ∼8 K.

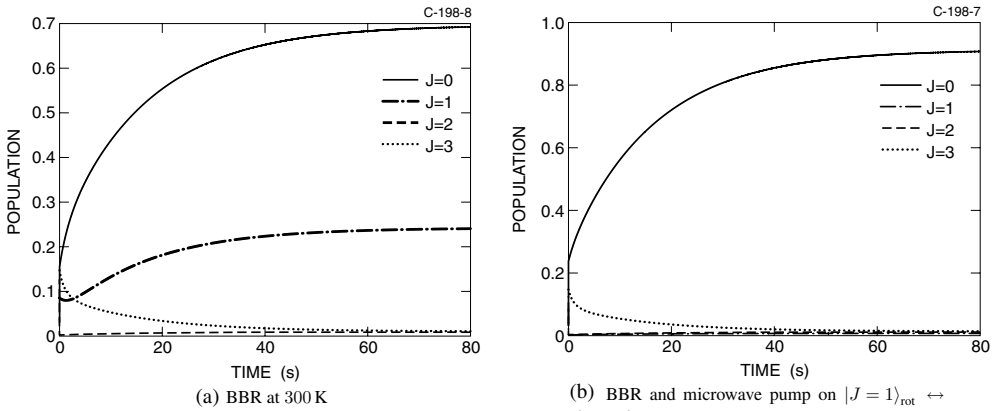

(a) BBR at 300 K

(b) BBR and microwave pump on $|J=1\rangle_{\text{rot}} \leftrightarrow |J=2\rangle_{\text{rot}}$

Figure 4. (a) Population in the four lowest rotational states of MgH^+ as a function of time, when subject to the 300 K BBR field present in the trap and the cooling scheme shown in figure 1 and using an excited vibrational state within the ground electronic state as an intermediate state in the Raman transition. The simulation was performed using effective rates for the pumping of population between $|J=0\rangle_{\text{rot}}$ (full curve) and $|J=2\rangle_{\text{rot}}$ (dashed curve) as explained in the text. (b) As (a) but with a microwave source (Lewen *et al* 1998) saturating the $|J=1\rangle_{\text{rot}} \leftrightarrow |J=2\rangle_{\text{rot}}$ transition.

6. Complications and prospects for improvements

The parameters used in section 4 are somewhat problematic when it comes to an experimental implementation. Most importantly, the assumed linewidth of the laser is very small. Furthermore, incoherent scattering on an intermediate state with linewidth of more than 10 MHz will be a problem. Thus, the achilles' heel of the scheme is incoherent scattering on the intermediate state, since scattering will take place on the dominant carrier transition, while the Raman transition must take place on sideband transitions for the scheme to be effective. The disadvantage was minimized by cooling with $^{40}Ca^+$, which results in a motionally cold sample. A modification of the cooling scheme may circumvent the problems with incoherent scattering on the intermediate state. First, the Raman transition could be changed to a stimulated Raman adiabatic passage (STIRAP) type transition. STIRAP transitions are generally robust, but driving selective sideband transitions in a trap with STIRAP is not straightforward. STIRAP on sideband transitions are discussed in another context by Vogelius *et al* (2006).

In the simulations presented, we assumed an oscillation frequency $\Omega_{\text{Ca}} = 50$ MHz for the calcium ion. Further simulations show that the scheme would indeed work for lower oscillation frequencies, but with a lower efficiency, other parameters being equal. Though at present a frequency of 50 MHz is relatively high for most ion traps, with the current focus on development of micro-traps (Stick *et al* 2006, Seidelin *et al* 2006), frequencies of this size may become standard in the near future.

When side-band laser cooling on the atomic ion is feasible it can lead to nearly exclusive population of the ground state of the collective mode of interest (without the laser field driving the transition in the molecular ion being present). Since this situation only requires a first-order Raman side-band molecular transition, generally much lower laser powers are needed and incoherent light scattering due to electronic excitation of the molecule can be made very small. As a consequence, a more effective rotational cooling will be expected

in this case. Experimentally, the drawback of side-band laser cooling is that this cooling is technically much more challenging than Doppler cooling. Another approach would be to use an excited vibrational state within the electronic ground state potential energy curve as intermediate state in the Raman transition. The narrow linewidth of such states would allow for smaller detunings and higher free-molecule Rabi frequencies in the Raman transition without inducing incoherent scattering. The trade-off would be that internal transitions typically have infrared transition frequencies, thus resulting in a very small Lamb–Dicke parameter. We have performed investigations along the latter lines using the first excited vibrational state of MgH^+ as intermediate state. The results show that this approach is feasible. In the simulation, we assumed the intermediate state to have a spontaneous decay rate of 50 Hz and a transition wavelength of 4 μm. The detuning from the excited state in the Raman process was 500 MHz, the molecular Rabi frequencies $\Omega^+_{\mathrm{mol}_1}$ and $\Omega^-_{\mathrm{mol}_2}$ of equation (28) were both 800 MHz and the lasers in the Raman process were tuned to resonance when $\nu'_p - \nu_p = 3$. The linewidth, Γ, of the Lorentzian in equation (28) was 100 kHz. The remaining parameters were identical to the ones used above. With these parameters, the rate of inhomogeneous scattering on the intermediate state was acceptable at 30 Hz. Figure 4 shows the cooling efficiency with these parameters. We have also included a simulation, where the $|J = 1\rangle_{\mathrm{rot}} \leftrightarrow |J = 2\rangle_{\mathrm{rot}}$ rotational transition is saturated with an additional microwave source (Lewen *et al* 1998). It appears that cooling using the scheme of figure 1 may be possible if the intermediate state in the molecular transition is long-lived.

7. Conclusion

In our proposal, we used internal–external state couplings to rotationally cool a molecular ion confined in a harmonic trap with a laser-cooled atomic ion. The only dissipative term in the cooling cycle stems from the spontaneous decay in the translational cooling of the atomic ion and it makes no reference to molecular vibrational structure, decay rates or selection rules. The scheme is hence fundamentally different from the previously proposed schemes (Vogelius *et al* 2002, 2004a, 2004b) in which the dissipative process was spontaneous decay from an excited molecular vibrational state.

The cooling scheme relies on cooling of the collective translational state through the atomic cooling cycle and pumping between an excited rotational molecular state and the molecular ground state with effective pumping rates faster than the rotational redistribution mediated by black-body radiation (BBR). The fundamental requirement of the scheme can therefore be summarized as $\gamma_{2\to 0} \gg \gamma_{\mathrm{BBR}}$, where the last rate is the rotational redistribution rate in BBR and $\gamma_{2\to 0}$ describes the effective pumping rate from $J = 2$ to $J = 0$ and is found from the rates of external cooling, $\{\Gamma_{\mathrm{atom}}\}$, and rates of the individual Raman transitions, $\{\Gamma_{\mathrm{mol}}\}$. Finally, γ_{BBR} must be much greater than the rate of trap loss. The method is versatile and may be adapted to polyatomic molecules, provided the rotational and, if relevant, vibrational redistribution due to BBR can occur from any populated state to the state addressed by the Raman laser on the required timescale.

For simplicity, we only considered Raman transitions where both the ground electronic potential and the excited potential to which the single Raman pulse couples are of Σ symmetry. If, however, one could couple to an excited state of different symmetry, say Π symmetry, the dipole selection rules would allow us to drive Raman transitions where the change in the rotational quantum number could be $\Delta_J = -1$. In such a case, one would therefore be able to avoid population of states other than the ground rotational state by letting the Raman transition be resonant with the $J = 1 \to J = 0$ transition. The drawback of coupling to a excited electronic potential with Π symmetry is though that such electronic potential curves

generally lie higher in energy than the first excited potentials of Σ symmetry, and are hence more difficult to reach by reasonable laser wavelengths.

Acknowledgments

LBM was supported by the Danish Natural Science Research Council (grant no 21-03-0163) and the Danish Research Agency (grant no 2117-05-0081). MD is supported by the Danish Natural Science Research Council, the Danish National Research Foundation through the Quantum Optics Center QUANTOP and by the Carlsberg Foundation.

References

Babab T and Waki I 1996 *Japan. J. Appl. Phys.* **35** L1134
Bertelsen A, Jørgensen S and Drewsen M 2006 *J. Phys. B: At. Mol. Opt. Phys.* **39** L83
Bethlem H and Meijer G 2003 *Int. Rev. Phys. Chem.* **22** 73
Blythe P, Roth B, Fröhlich U, Wenz H and Schiller S 2005 *Phys. Rev. Lett.* **95** 183002
Cirac J I and Zoller P 1995 *Phys. Rev. Lett.* **74** 4091
Doyle J *et al* 2004 *Eur. Phys. J.* D **31** 149
Drewsen M, Mortensen A, Martinussen R, Staanum P and Sørensen J L 2004 *Phys. Rev. Lett.* **93** 243201
Egorov D *et al* 2002 *Phys. Rev.* A **66** 043401
James D 1998 *Appl. Phys.* B **66** 181–90
Kielpinski D *et al* 2000 *Phys. Rev.* A **61** 032310
Leibfried D *et al* 2003 *Nature (London)* **422** 412
Lewen F *et al* 1998 *Rev. Sci. Instrum.* **69** 32 (see also www.istok.com)
Metcalf H J and van der Straten P 1999 *Laser Cooling and Trapping* (Berlin: Springer)
Mølhave K and Drewsen M 2000 *Phys. Rev.* A **62** 011401(R)
Monroe C, Meekhof D M, King B E, Jefferts S R, Itano W M, Wineland D J and Gould P 1995 *Phys. Rev. Lett.* **75** 4011
Seidelin S *et al* 2006 *Preprint* quant-ph/0601173
Schmidt-Kaler F, Häffner H, Riebe M, Gulde S, Lancaster G P T, Deuschle T, Becher C, Roos C F, Eschner J and Blatt R 2003 *Nature (London)* **422** 408
Sørensen A and Mølmer K 1999 *Phys. Rev. Lett.* **82** 1971
Stick D, Hensinger W K, Olmschenk S, Madsen M J, Schwab H and Monroe C 2006 *Nature Phys. (London)* **2** 36
van Eijkelenborg M A, Storkey M E M, Segal D M and Thompson R C 1999 *Phys. Rev.* A **60** 3903
Vogelius I S, Madsen L B and Drewsen M 2002 *Phys. Rev. Lett.* **89** 173003
Vogelius I S, Madsen L B and Drewsen M 2004a *Phys. Rev.* A **70** 053412
Vogelius I S, Madsen L B and Drewsen M 2004b *J. Phys. B: At. Mol. Opt. Phys.* **37** 4571–4
Vogelius I S, Madsen L B and Drewsen M 2006 *J. Phys. B: At. Mol. Opt. Phys.* **39** S1259 (*Preprint* physics/057181)
Wineland D J and Itano W M 1979 *Phys. Rev.* A **20** 1521–40